

Sequential phosphorylation and multisite interactions characterize specific target recognition by the FHA domain of Ki67

In-Ja L Byeon^{1,5}, Hongyuan Li^{2,5}, Haiyan Song², Angela M Gronenborn^{1,3} & Ming-Daw Tsai^{2,4}

The forkhead-associated (FHA) domain of human Ki67 interacts with the human nucleolar protein hNIFK, recognizing a 44-residue fragment, hNIFK_{226–269}, phosphorylated at Thr234. Here we show that high-affinity binding requires sequential phosphorylation by two kinases, CDK1 and GSK3, yielding pThr238, pThr234 and pSer230. We have determined the solution structure of Ki67FHA in complex with the triply phosphorylated peptide hNIFK_{226–269}3P, revealing not only local recognition of pThr234 but also the extension of the β -sheet of the FHA domain by the addition of a β -strand of hNIFK. The structure of an FHA domain in complex with a biologically relevant binding partner provides insights into ligand specificity and potentially links the cancer marker protein Ki67 to a signaling pathway associated with cell fate specification.

The human Ki67 protein was originally identified as the antigen for the monoclonal antibody Ki67 generated against a Hodgkin lymphoma cell line in the early 1980s^{1,2}. Ki67 antibodies have been used extensively as a prognostic and diagnostic tool in histopathology because the presence of the Ki67 antigen is stringently related to cell proliferation; it is observed in the nuclei of dividing cells in the G1, S and G2 phases and in mitosis, but not in the G0 phase of quiescent cells³. Despite the widespread use of Ki67 antibodies, remarkably little is known about the biological function of the antigen⁴. Only a few functional studies have been reported in the past decade^{5–8}.

The sequence organization of Ki67 reveals an FHA domain at its N terminus, shown to be a ubiquitous, modular phosphopeptide-binding domain^{9–14}. A SMART database search¹⁵ allowed the identification of at least 708 FHA domains (99 for human proteins) in very functionally diverse proteins. At the present time, two proteins have been shown by pull-down experiments to interact with the FHA domain of Ki67 in a mitosis- and phosphorylation-dependent manner: human kinesin-like protein-2 (Hklp2)¹⁶ and hNIFK¹⁷. In the latter interaction, Thr234 and Thr238 have been implicated as possible phosphorylation sites by mutagenesis¹⁷. In addition, *in vivo* studies using immunofluorescence microscopy revealed colocalization of hNIFK and Ki67 at particular sites of mitotic chromosomes¹⁷.

We recently solved the solution structure of the FHA domain of Ki67 (ref. 18). Notably, in contrast to other FHA domains that bind tightly to one or more short phosphopeptides (8–15 residues) containing pTXX(D/I/L) motifs or SQ/TQ clusters, we found that

Ki67FHA does not bind tightly to short phosphopeptides. Instead, we observed tight binding of Ki67FHA to a much larger peptide, a 44-residue fragment of hNIFK, hNIFK_{226–269}(pThr234), that was phosphorylated at Thr234. Using chemical shift perturbation, the binding surface on Ki67FHA was mapped by ¹H,¹⁵N heteronuclear single quantum coherence (¹H-¹⁵N HSQC) spectroscopy¹⁸.

Although FHA domains have been extensively studied in recent years^{9–12,18–26}, no structure of an FHA domain in complex with a biological binding partner has thus far been reported. All structures now available show uncomplexed FHA domains or complexes with very short phosphopeptides, primarily derived from peptide library screens. Even in those cases in which the bound peptide corresponds to a sequence of a biological binding partner, no direct evidence for the importance of this site for *in vivo* activity exists. Although binding partners have been identified at the cellular level for some FHA domains in the past two years^{19,21}, difficulties in the preparation of the correctly phosphorylated proteins have made structural characterization of FHA–phosphoprotein complexes challenging. Here, we have determined the structure of the complex between Ki67FHA and hNIFK_{226–269}3P to provide insight into the crucial determinants for the FHA–phosphoprotein interactions.

RESULTS

Sequential phosphorylation of hNIFK by CDK1 and GSK3

hNIFK_{226–269} (KTVDSQGPTPVCTPTFLERRKSQVAELNDDDKDDEIVFKQPISC), was expressed as a fusion construct in *Escherichia coli*, and isotope-labeled peptide was prepared for NMR studies.

¹Laboratory of Chemical Physics, National Institute of Diabetes and Digestive and Kidney Diseases, US National Institutes of Health (NIH), Bethesda, Maryland 20892, USA. ²Departments of Chemistry and Biochemistry and Ohio State Biochemistry Program, The Ohio State University (OSU), Columbus, Ohio 43210, USA. ³Program in Structural Biology, University of Pittsburgh School of Medicine, Pittsburgh, Pennsylvania 15261, USA. ⁴Genomics Research Center, Academia Sinica, Taipei 115, Taiwan. ⁵These authors contributed equally to this work. Correspondence should be addressed to A.M.G. (amg100@pitt.edu) or M.-D.T. (tsai.7@osu.edu).

Received 13 June; accepted 22 September; published online 23 October 2005; doi:10.1038/nsmb1008

Enzymatic methods were used for phosphorylation, rather than synthetic ones commonly used in peptide studies.

Because earlier work had implicated Thr234 and possibly Thr238 in hNIFK as important residues in the interaction between Ki67FHA and hNIFK^{17,18}, we searched for kinase target motifs containing threonine (<http://scansite.mit.edu>). A search of all possible sequences using high and medium stringency yielded no hits. At low stringency, however, we identified Thr234 and Thr238 as possible phosphorylation targets for GSK3, and Thr238 as a potential substrate for CDK1. Tests with CDK1 were initially conducted using a radiolabel-based assay, where hNIFK_{226–269} behaved comparably to a peptide derived from histone H1, the standard substrate of CDK1. Mass spectrometry (MS) analyses indicated a single phosphorylation, and the amino acid target of phosphorylation was identified as Thr238 by mutagenesis.

Initially, no phosphorylation by either GSK3 α or GSK3 β was observed for any of the putative sites. Given that GSK3 can uniquely recognize a priming phosphoryl group at +4 serine or threonine²⁷, we tested for the possibility that phosphorylation of Thr234 by GSK3 proceeds only after Thr238 is already phosphorylated by CDK1. Such double phosphorylation was indeed observed and confirmed by MS and mutagenesis. Only a single residue, Thr238, became phosphorylated in the T234A mutant of hNIFK_{226–269} when both kinases were used. In addition, extended incubation with both kinases resulted in a triply phosphorylated product. We speculated that Ser230 might be the third residue and confirmed this proposal by mutagenesis. Phosphorylation of hNIFK_{226–269} S230A by both kinases resulted only in double phosphorylation (Supplementary Table 1 online). Therefore, our results clearly establish that GSK3 can phosphorylate Thr234 in the presence of phosphorylated Thr238 and that Ser230 becomes phosphorylated only after Thr234. Judging qualitatively from the extent of phosphorylation, GSK3 α and GSK3 β phosphorylated Thr234 in hNIFK_{232–269} similarly to phospho-glycogen synthase peptide-2, whereas Ser230 was phosphorylated less efficiently. As described in Supplementary Figure 1 online, phosphorylation by use of cell lysate in the presence and absence of specific kinase inhibitors supports the biological relevance of these phosphorylation events, but additional *in vivo* studies are required.

The triply phosphorylated hNIFK_{226–269}, referred to as hNIFK_{226–269}3P, bound to Ki67FHA slightly more tightly than the

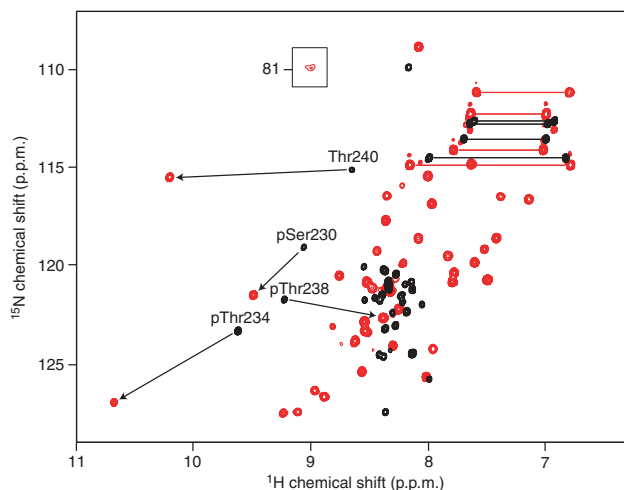


Figure 1 ¹H-¹⁵N HSQC spectra of hNIFK_{226–269}3P free (black) and in complex with Ki67FHA (red). The latter sample contained 0.9 mM ¹³C, ¹⁵N-hNIFK_{226–269}3P and 1 mM unlabeled Ki67FHA. Resonances for all three phosphorylated residues (pSer230, pThr238 and pThr234) and Thr240 are labeled at their free positions and connected by arrows to those of the bound form. Pairs of signals corresponding to side chain amino groups of Asn and Gln are connected by black (free peptide) and red (complex) lines. The insert shows the N ϵ H side chain resonance of Arg245.

doubly phosphorylated peptide (see below) and was used to determine the structure of the complex. The binding modes of both phosphopeptides are essentially identical, as judged by a comparison of the ¹H-¹⁵N HSQC spectra of the two complexes, and interpretation of the structural results will be applicable to the biological data obtained primarily on the doubly phosphorylated peptide.

Regulation of phosphorylation by adjacent prolines

Three proline residues are present near the phosphorylation sites, namely Pro233, Pro235 and Pro239. Cell cycle-related kinases such as CDKs and mitogen-activated protein kinase generally recognize Thr/Ser-Pro motifs. To evaluate the role of the prolines in hNIFK in phosphorylation, we constructed single proline-to-alanine mutants, P233A, P235A and P239A, and tested their phosphorylation by the two kinases. Evaluation of the phosphorylation reaction by MS (Supplementary Table 1) revealed that the P239A mutation reduced phosphorylation at both Thr238 and Thr234 from 91% and 53%, respectively, to 10% and 4%, respectively, whereas the P235A mutation lowered the phosphorylation at Thr234 by GSK3 from 53% to 18%. Therefore, it seems that Pro239 is required for the phosphorylation of Thr238 by CDK1 and that Pro235 influences the phosphorylation of Thr234 by GSK3 in hNIFK. Most notably, it was observed that the mutant P233A could be doubly phosphorylated (at Thr238 and Thr234) by CDK1. Thus the presence of a proline at position 233 impedes Thr234 phosphorylation by CDK1.

The intricate regulatory effects of the three proline residues on the phosphorylation of Thr238 and Thr234 suggest that ordered phosphorylations by the two kinases are probably biologically relevant events. If verified *in vivo*, such sequential phosphorylation may represent an important mechanism for switching between different partners in protein-phosphoprotein interactions.

Determination of binding affinities for hNIFK and Ki67FHA

Dissociation constants (K_d) for the Ki67FHA-hNIFK_{226–269} complexes were determined using surface plasmon resonance (SPR) (Table 1).

Table 1 Dissociation constants of the Ki67FHA-hNIFK_{226–269} complexes determined by SPR

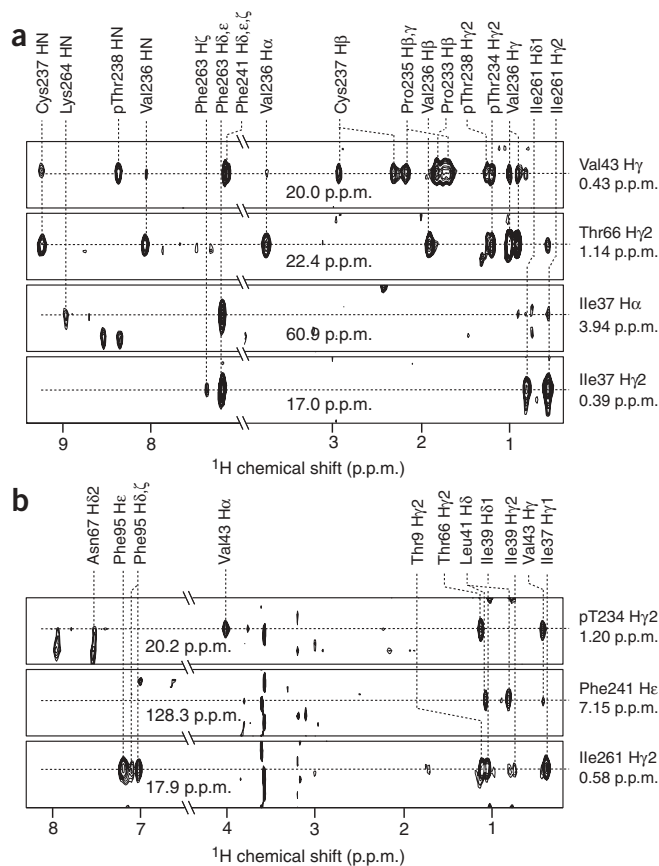
Row no.	hNIFK variants	Phosphorylation sites	K_d (μ M) of FHA-hNIFK	K_d ratio ^a
1	hNIFK _{226–269}	230, 234, 238	0.077 \pm 0.009	1.0
2	S230A	234, 238	0.17 \pm 0.01	2.3
3	T234A	238	131 \pm 6	1,700
4	hNIFK _{226–269}	None	109 \pm 12 ^b	1,420
5	T234S	230, 234, 238	5.5 \pm 0.9	71
6	P233A	230, 234, 238	0.085 \pm 0.009	1.1
7	P235A	230, 234, 238	0.34 \pm 0.02	4.4
8	V236A	230, 234, 238	0.40 \pm 0.03	5.3
9	C237A	230, 234, 238	0.25 \pm 0.05	3.2
10	F241A	230, 234, 238	2.4 \pm 0.4	31
11	hNIFK _{226–259}	230, 234, 238	14 \pm 4	180
12	hNIFK _{260–266} , heptapeptide	None	42,000 \pm 5,000 ^b	550,000

^aCompared to triply phosphorylated hNIFK_{226–269}.

^bThe K_d values of these weak binding complexes were measured by ¹H-¹⁵N HSQC NMR.

Figure 2 Intermolecular NOEs observed for the Ki67FHA–hNIFK_{226–269}3P complex from 3D ¹³C-edited, ¹²C/¹⁴N-filtered NOE spectra.

(a) Representative NOEs using a sample containing ¹³C,¹⁵N-labeled Ki67FHA and unlabeled hNIFK_{226–269}3P. (b) Representative NOEs using a sample containing ¹³C,¹⁵N-labeled hNIFK_{226–269}3P and unlabeled Ki67FHA. Spectra were recorded at 500 MHz in H₂O. The ¹³C chemical shifts of each selected strip are shown inside panels.



hNIFK_{226–269}3P bound tightly to Ki67FHA, with a K_d value of 0.077 μ M, and the doubly phosphorylated S230A mutant showed only slightly weaker binding. Binding was also observed by ³¹P NMR (Supplementary Fig. 2 online); large chemical shift differences between the free and bound forms were observed for the ³¹P resonances of pThr234 and pThr238, but not pSer230. This suggests that pThr234 and pThr238 undergo substantial changes in environment upon binding Ki67FHA, with pSer230 being less affected. It should be noted, however, that even unphosphorylated hNIFK_{226–269} was able to bind specifically to Ki67FHA, albeit very weakly ($K_d = 109 \mu$ M), as was the T234A mutant with single phosphorylation at Thr238 ($K_d = 131 \mu$ M). The binding data indicate that phosphorylation at Thr234 contributes substantially, that at Ser230 marginally and that at Thr238 not at all to the overall affinity. The structural bases for the observed binding affinities are described in the next sections.

hNIFK_{226–269}3P becomes structured by Ki67FHA binding

In the ¹H-¹⁵N HSQC spectrum of the free ¹³C,¹⁵N-hNIFK_{226–269}3P peptide (Fig. 1, black contours), the amide resonances of the phosphorylated residues, pSer230, pThr234 and pThr238, were all substantially downfield shifted, consistent with known shift effects of phosphorylation. However, the small spectral dispersion of all other backbone ¹HN resonances (7.9–8.5 p.p.m.) clearly indicated that the peptide is essentially unstructured. Upon interaction with Ki67FHA (Fig. 1, red), all resonances showed substantially increased chemical shift dispersion (7.0–10.2 p.p.m.), indicating that the random-coiled peptide adopts a well-defined structure. Notably, in the bound peptide, the NεH side chain resonance of Arg245 was easily observed (9.02/81.0 p.p.m.; ¹H/¹⁵N), whereas in the free peptide fast exchange

with water rendered it undetectable. This clearly shows that the NεH proton is buried in the complex.

Loss of conformational heterogeneity of Ki67FHA

In the ¹H-¹⁵N HSQC spectrum of Ki67FHA not in complex, several backbone ¹H-¹⁵N HSQC resonances were broadened beyond detection on account of conformational exchange on the micro- and millisecond time scale¹⁸. Upon hNIFK_{226–269}3P binding, the conformational equilibrium shifted toward a unique conformation, rendering all resonances observable. In addition, the ¹H-¹⁵N HSQC spectrum of ¹³C,¹⁵N-Ki67FHA in complex with hNIFK_{226–269}3P was very similar to that in complex with the singly phosphorylated synthetic peptide¹⁸ except for the Gly32, Glu34, Ile39 and Gln40 resonances, suggesting that these amino acids interact with the two additional pSer230 and/or pThr238 phosphate groups. The more likely candidate for the interactions is pSer230, because binding to Ki67FHA is enhanced 2.3-fold upon phosphorylation of this residue (Table 1).

NMR structure of the Ki67FHA–hNIFK_{226–269}3P complex

The solution structure of the Ki67FHA–hNIFK_{226–269}3P complex was determined on the basis of 3,476 NMR-derived constraints (3,141 distance, 215 dihedral angle and 120 N-H residual dipolar coupling constraints). Among these, a total of 320 intermolecular distance constraints were derived from a 3D ¹³C-edited, ¹²C/¹⁴N-filtered NOESY spectrum (Fig. 2).

The structure (Fig. 3) reveals that although the architecture of Ki67FHA in the complex is similar to that of free Ki67FHA (backbone N,C α ,C' atom pairwise r.m.s. deviation value 1.3 Å), notable differences in the loop conformations are present. The largest differences are observed for the β 1- β 2, β 5- β 6 and β 6- β 7 loops: in the free

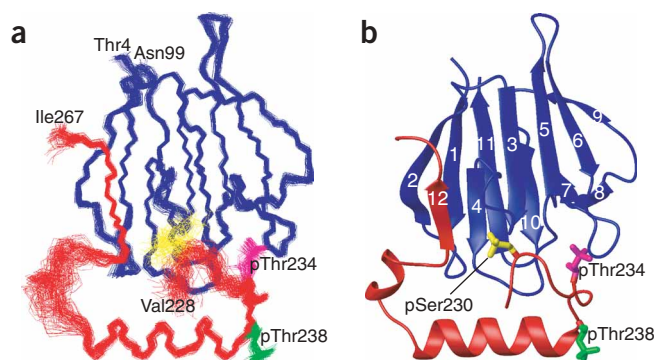


Figure 3 Overall structure of the Ki67FHA–hNIFK_{226–269}3P complex. (a) Superposition of the final ensemble comprising 100 conformers. Backbone atoms (N, C α , C') of Ki67FHA (residues 4–99) and hNIFK_{226–269}3P (residues 228–267) are shown in blue and red, respectively. Side chain atoms of the phosphorylated residues (pSer230 in yellow, pThr234 in magenta and pThr238 in green) are also included. (b) The ribbon diagram of a representative structure, colored as in a. β -strands are numbered, but note that numbering differs from that in reference 18.

state these regions are ill-defined, whereas they become structured in the complex. For hNIFK_{226–269}3P, on the other hand, a substantial conformational change between the free and bound structures occurs: residues 239–251 become α -helical and residues 260–264 adopt a β -strand conformation. Most notably, this β -strand extends the β -sheet of Ki67FHA, running antiparallel to β 4. Residues residing on the α -helix interact with the β 4– β 5 and β 10– β 11 loops of Ki67FHA. The peptide shows close packing against Ki67FHA and buries a large surface area of Ki67FHA (1,450 Å² of a total 6,037 Å²).

We took considerable care to establish the conformations of Pro233, Pro235 and Pro239, the three important proline residues in hNIFK_{226–269}3P near pThr234. For all three, the H δ but not H α protons showed strong NOEs to the H α of the preceding residue ($i - 1$), unambiguously establishing their peptide bond conformations as *trans*.

Local interactions around pT234

Detailed interactions in the binding interface between Ki67FHA and hNIFK_{226–269}3P are depicted in **Figure 4**, and the region around pThr234–Cys237 is shown in **Figure 4a**. Previous binding and structural studies on FHA with short pThr peptides have implicated residues immediately after the phosphothreonine in the interaction. In the present structure, the pThr234 phosphate forms hydrogen bonds with the side chains of Arg31, Ser45, Lys46 and Thr66 and the backbone HN of Lys46. This hydrogen-bonding network extends to the conserved His48 residue in FHA, with the Ser45 backbone NH donating a hydrogen bond to the imidazole N δ . The tautomeric states of all histidines in Ki67FHA were determined by heteronuclear multiple-bond correlation spectroscopy, verifying that the imidazole ring N ϵ of His48 is protonated.

Although it is well accepted that FHA domains recognize pThr and not pSer, the present system allowed a quantitative assessment of the pThr versus pSer specificity. Replacement of Thr234 by serine resulted in a reduction in affinity by a factor of 71 (**Table 1**), indicating that the van der Waals interactions of Thr234–C γ H₃ with Val43, Thr66 and Asn67 from Ki67FHA add a considerable fraction of the binding energy (**Figs. 2b** and **4a**).

Residues at the +1 to +3 positions after pThr234 are involved in backbone–side chain hydrogen-bonding interactions with residue Asn67. In particular, the backbone carbonyl oxygen of Pro235 (+1 position) accepts a hydrogen bond from the Asn67 H δ 2 proton, whereas the amide proton of Cys237 (+3 position) donates one to the Asn67 O δ 1 oxygen. In addition, the Asn67 N δ 2H₂ amino group donates an additional hydrogen bond to the Val43 carbonyl oxygen. For the +3 residue (Cys237), only limited hydrophobic interactions with Val43 and Ile91 are present, and no hydrogen bonds between the S γ H group and residues on the FHA domain are observed.

The emerging picture from our structure is quite distinct from that suggested for other FHA domains: for the latter, the pThr+3 residue is thought to be the most important determinant for ligand specificity, on the basis of screens of short phosphopeptide libraries, which identified the pTXX(D/I/L) motif (also called the pThr +3 rule)^{9,11,12,24–26,28}. Notably, Ki67FHA did not show any preference in these studies¹⁸. Using the longer phosphopeptide fragment, hNIFK_{226–269}, allowed us to test whether any residues around pThr234 are involved in the interaction with Ki67FHA. Mutants P233A, P235A, V236A and C237A were generated and converted into their triply phosphorylated forms. Binding of these variants to Ki67FHA (**Table 1**) shows that each of the alanine mutations in the –1 to +3 residues reduced the binding affinity by less than a factor of 5. These modest effects are consistent with the structural data that show primarily backbone interactions.

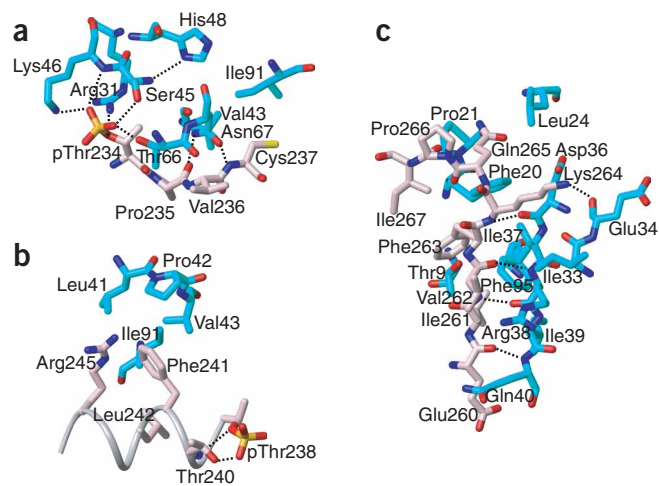


Figure 4 Intermolecular interactions between Ki67FHA and hNIFK_{226–269}3P. **(a)** Interactions involving pThr234 as well as +1, +2 and +3 residues of hNIFK. **(b)** Interface between the binding loops on Ki67FHA and the α -helix of hNIFK. **(c)** Interface between the β -strand of hNIFK and the β -sheet of Ki67FHA. For all interactions, carbon atoms are shown in cyan (FHA) or pink (hNIFK), nitrogen atoms in blue, oxygen atoms in red, sulfur atoms in yellow and phosphorus atoms in orange. Predicted hydrogen bonds are depicted with dashed lines.

Interactions involving the α -helix of hNIFK_{226–269}3P

The binding interface between the β 4– β 5 and β 10– β 11 loops of Ki67FHA and the α -helix of hNIFK peptide (**Fig. 4b**) creates a new, intermolecular hydrophobic core in the complex. Leu41, Pro42 and Val43 in the β 4– β 5 loop and Ile91 in the β 10– β 11 loop form a hydrophobic patch into which Phe241, Leu242 and Arg245 of the hNIFK peptide insert. It is especially noticeable that these β 4– β 5 loop residues are all hydrophobic, in contrast to other FHA domains, where at least two of the three residues are polar¹⁸. Immersion into the completely hydrophobic patch may contribute to the stabilization of the α -helical conformation for this region of the hNIFK peptide. It should be emphasized that the structure under discussion is the first structure of an FHA–pThr phosphopeptide complex to show this type of extended interaction beyond the pThr234 recognition. No interaction of the second phosphothreonine, pThr238, with the FHA domain is observed. Instead, intramolecular hydrogen bonds within hNIFK, such as those between the phosphate of pThr238 and the backbone NH and the side chain O γ H of Thr240, are used to stabilize the helical conformation. This interaction explains the notable downfield shift of the Thr240 backbone NH resonance upon Ki67FHA binding (**Fig. 1**).

The importance of the hydrophobic contact between hNIFK Phe241 and Ki67FHA Val43 was examined by site-directed mutagenesis. The binding affinity was reduced by a factor of 31 for the F241A mutant (**Table 1**), suggesting a large contribution of this interaction to the binding energy. A less dramatic reduction (5.6-fold increase in K_d) was observed for the V43I mutant, in which the size of the hydrophobic side chain is increased by one methylene group, probably causing some steric clash.

Interactions involving the β -strand of hNIFK

A new interface involving residues 260–264 of hNIFK_{226–269}3P is formed upon binding to Ki67FHA (**Fig. 4c**). This stretch of peptide forms a β -strand that adds to one edge of the Ki67FHA β -sheet, extending the overall β -sheet structure by aligning antiparallel to β 4. In addition to the canonical β -sheet hydrogen bonds, many

hydrophobic interactions between side chains are observed. In particular, Ile261, Val262 and Phe263 interact with Ile37, Arg38 and Ile39 (β 4), Ile33 (loop β 3- β 4), Phe20 (β 2), Thr9 (β 1) and Phe95 (β 11) of FHA.

Intrigued by the observation of the β -strand addition of hNIFK to the Ki67FHA β -sheet, we evaluated the contribution of this interaction to the overall binding. The SPR data (Table 1, row 11) indicated that binding for a peptide lacking this interaction is reduced 180-fold, clearly showing its importance. We also investigated whether a heptapeptide (residues 260–266) alone was capable of binding to Ki67FHA. Binding was probed by ^1H - ^{15}N HSQC (Supplementary Fig. 3 online). The largest chemical shift changes in the spectrum of Ki67FHA were observed for residues on β 4 (Ile37, Arg38, Ile39 and Gln40). Other affected residues, such as Val15 and Ser94, are located near the hNIFK β -strand in the structure. Furthermore, the trend observed for the changes in resonance positions are similar to that seen with the parent peptide, hNIFK_{226–269}3P. This clearly shows that the heptapeptide interacts at the same site as does hNIFK_{226–269}, although the binding is extremely weak ($K_d = 42 \pm 5$ mM, Table 1).

DISCUSSION

The structure of the Ki67FHA–hNIFK_{226–269}3P complex reveals the participation of several sites as well as an intricate and intimate relationship between the binding partners. Although both Ki67FHA and hNIFK_{226–269}3P are portions of larger proteins, it is probable that the interactions we observed are representative of those *in vivo* of the full-length proteins, given their modular nature. Our phosphorylation studies showed that GSK3 phosphorylates Thr234 only in the context of phosphorylated Thr238. In addition, three proline residues located around the crucial phosphothreonine show interesting regulatory effects, possibly acting as a molecular switch. Therefore, phosphorylation at Thr234 of hNIFK and its specific recognition by Ki67, after priming phosphorylation of Thr238 by CDK1, are probably important cellular events. Both our structural and functional results are highly consistent and can direct additional studies aimed at explaining the overall interaction between these two proteins.

We have previously suggested that the binding recognition of FHA domains involves three main components (the pThr residue, residues at the +1 to +3 positions and an extended binding surface) and that variability in these three factors causes the amazing diversity in the function and specificity of FHA domains from different sources¹⁸. In this study, we show that the phosphothreonine and a completely ordered, extended binding surface are most important, whereas the +1 to +3 residues contribute only moderately to the Ki67FHA–hNIFK interaction. Notably, the novel binding interface between the two proteins involves extension of the β -sheet of Ki67FHA by a β -strand from hNIFK. Our data provide for the first time such a complete analysis for an FHA domain and suggest that it is important to study the interactions of other FHA domains with longer phosphopeptide fragments of the binding partner. In particular, our results indicate the necessity to reevaluate data on other signal transduction domains obtained with short peptide or phosphopeptide libraries. As shown for the Ki67FHA domain and the yeast Rad53FHA1 domain²⁹, information gleaned from such short peptides may be insufficient or even inaccurate.

Our functional results suggest that binding of hNIFK to Ki67FHA *in vivo* is probably regulated by the two master control kinases during mitosis, with hNIFK initially phosphorylated by the nuclear kinase CDK1 and subsequently by the cytosolic kinase GSK3. Because the Ki67 protein is located primarily in the perichromosomal area and migrates with chromosomes during cytokinesis, it is possible that

the interaction of Ki67 with phosphorylated hNIFK aids in equal partitioning between daughter cells. These possibilities are potential subjects for further *in vivo* studies.

METHODS

Expression and purification of hNIFK_{226–269}, mutants and Ki67FHA. A preScission protease site was engineered between the GB1 gene and hNIFK_{226–269} in pGBhNIFK_{226–269}¹⁸. The new plasmid, designated pGBhNIFK_{226–269}, was used to generate mutants. *E. coli* BL21 (DE3) Codon-Plus cells (Stratagene) were transformed with pGBhNIFK_{226–269}, and mutant plasmids and proteins were overexpressed as GB1 fusions with His-tag. Fusion proteins were purified over a nickel-NTA affinity column (Qiagen) followed by gel filtration on an S100 column (Amersham Pharmacia). The GB1 tag was cleaved by preScission protease (Amersham Pharmacia) and removed by reverse phase HPLC using a linear gradient (buffer A, 0.1% (v/v) trifluoroacetic acid (TFA) in water; buffer B, 0.1% (v/v) TFA in acetonitrile) on a C8 column (208TP510 from Vydac). Eluted hNIFK_{226–269} and mutants were lyophilized and stored at -20 °C. Ki67FHA was expressed and purified as described previously¹⁸. Site-directed mutagenesis was conducted using the QuikChange mutagenesis kit (Stratagene). PCR amplifications were done with pGBhNIFK_{226–269} as the template. Purified proteins were verified by MS.

***In vitro* phosphorylation.** Kinase reactions were carried out by adding 0.4 μ l of kinase (CDK1, GSK3 α or GSK3 β ; Upstate Cell Signaling Solutions, Inc.) to a 50- μ l reaction mixture (0.05 mM peptide, 1 mM ATP, 50 mM HEPES,

Table 2 Structural statistics for the Ki67FHA–hNIFK_{226–269}3P complex

	Ki67FHA	hNIFK _{226–269} 3P
NMR distance and dihedral constraints		
Distance constraints		
Total NOE	2,136	567
Intraresidue	611	253
Inter-residue	1,525	314
Sequential ($ i - j = 1$)	482	205
Nonsequential ($ i - j > 1$)	1,043	109
Hydrogen bonds	37 \times 2	10 \times 2
Ki67FHA–hNIFK _{226–269} 3P intermolecular	344	
Total dihedral angle constraints		
ϕ^a	71	21
ψ^a	67	24
Total N-H RDC constraints	87	33
Structural statistics (100 structures)		
Violations		
Distance constraints (Å)	0.016 \pm 0.016	0.019 \pm 0.005
Dihedral angle constraints (°)	0.315 \pm 0.086	0.231 \pm 0.192
Maximum dihedral angle violation (°)	5	5
Maximum distance violation (Å)	0.4	0.4
Deviations from idealized covalent geometry		
Bond lengths (Å)	0.0028 \pm 0.0003	0.0027 \pm 0.0003
Bond angles (°)	0.550 \pm 0.015	0.564 \pm 0.025
Improper (°)	0.460 \pm 0.019	0.518 \pm 0.030
R.m.s. deviations from the average structure (Å) ^b		
Backbone atoms	0.40 \pm 0.05	0.40 \pm 0.05
All heavy atoms	0.81 \pm 0.05	1.07 \pm 0.10

^a ϕ and ψ constraints were obtained using TALOS³⁶.

^bR.m.s. deviations from the average structure were calculated for the final 100 structures by excluding flexible, poorly defined regions (Ki67FHA residues 1–3 and 100–120; and hNIFK residues 226–230, 253–258, 268 and 269).

10 mM MgCl₂, 5 mM DTT, 1 mM EGTA and 0.01% (v/v) Brij35 (pH 7.4) at 25 °C) and incubating at 30 °C for 1 h. The extent of phosphorylation was assessed by electrospray ionization MS. Radioactive kinase assays were carried out by adding 5 μCi (ICN, ~10 mCi ml⁻¹, ~25 Ci mmol⁻¹) of [γ -³²P]ATP to 20 μl of a preincubated reaction mixture (no ATP) with 0.4 U of CDK1 for 15 min. The reaction was quenched by adding SDS-PAGE loading buffer. After electrophoresis, the intensities of bands were determined using a Phosphor-Imager (Amersham Pharmacia).

Preparation of phosphorylated hNIFK_{226–269} and mutants for structural and functional studies. A 20-mg aliquot of hNIFK_{226–269} was incubated with 10 U of CDK1 in 5 ml of reaction buffer (6 mM ATP, 50 mM HEPES, 10 mM MgCl₂, 5 mM DTT, 1 mM EGTA and 0.01% (v/v) Brij35 (pH 7.4) at 25 °C) for 24 h. Under these conditions, hNIFK_{226–269}PThr238 was the major reaction product. The singly phosphorylated peptide was purified by HPLC and its identity verified by MS. Triply phosphorylated hNIFK_{226–269}3P was prepared in equivalent fashion using hNIFK_{226–269}PThr238 as the substrate and GSK3β as the kinase.

Determination of the dissociation constants by SPR. hNIFK_{226–269} and mutants were biotinylated with sulfo-NHS-biotin (Pierce), diluted to 1 μM with eluent buffer (5 mM HEPES, 5 mM DTT, 1 mM EDTA and 150 mM NaCl (pH 7.4)) and immobilized on sensorchip SA (BIAcore). Biotinylated BSA was used as a control and was immobilized in the control channels. Sensorgrams were measured on a Biacore 3000 instrument for a series of concentrations (0.01 μM to ~50 μM) of Ki67FHA by injecting (20 μl min⁻¹ for 1 min) into the sensorchip flow channels at 25 °C. Responses were fit to a hyperbola function $RU = c \times RU_{\max} / (K_d + c)$, where RU is the response unit change, RU_{\max} the maximal response unit change, K_d the dissociation constant and c the protein concentration.

Titration experiments by NMR. All NMR spectra were recorded at 17 °C on protein samples in 5 mM HEPES buffer containing 5 mM DTT, 1 mM EDTA and 150 mM NaCl (pH 7.4) on a Bruker DRX600 spectrometer. Binding of phosphorylated hNIFK_{226–269} to ¹⁵N-labeled Ki67FHA was followed by recording ¹H-¹⁵N HSQC spectra until saturation was reached. Binding of Ki67FHA to phosphorylated hNIFK_{226–269} S230A was followed by ³¹P NMR.

NMR structure determination of the Ki67FHA–hNIFK_{226–269}3P complex. All NMR spectra of the complex were recorded at 17 °C on two samples: one contained 0.9 mM ¹³C,¹⁵N-Ki67FHA and 1 mM unlabeled hNIFK_{226–269}3P and the other 0.9 mM ¹³C,¹⁵N-hNIFK_{226–269}3P and 1 mM unlabeled Ki67FHA in 5 mM HEPES, 5 mM DTT, 1 mM EDTA and 150 mM NaCl (pH 7.4). The hNIFK_{226–269}3P peptide contains four extra residues (Gly-Pro-Gly-Ser) at the N terminus and eight extra residues (LEHHHHHH) at the C terminus as fusion tag artifacts. Spectra were recorded on Bruker DRX800, DMX750, DRX600, DMX600 or DMX500 spectrometers equipped with 5-mm triple-resonance, three-axes gradient probes or z-axis gradient cryoprobes. Assignments for the 20.8-kDa complex were achieved (100% backbone and >98% side chain) using 3D HNCACB, CBCA(CO)NH, HCCH-TOCSY and ¹³C-edited and ¹⁵N-edited NOESY experiments^{30,31}. Interproton distance restraints were derived from 3D ¹³C-edited, ¹⁵N-edited and ¹³C-edited/¹²C,¹⁴N-filtered NOESY experiments (mixing time 100 ms)^{32,33}. Spectra were processed with NMRPipe³⁴ and analyzed using NMRDraw and PIPP, CAPP and STAPP³⁵. Approximate interproton distance restraints were grouped into four ranges: 1.8–2.7 Å, 1.8–3.3 Å, 1.8–5.0 Å and 1.8–6.0 Å, corresponding to strong, medium, weak and very weak NOEs, respectively. In addition, 0.5 Å was added to the upper limit of interproton distance restraints involving methyl groups. For hydrogen bonds, distance constraints of 1.5–2.5 Å (H-O) and 2.5–3.5 Å (N-O) were used. Backbone torsion angle (ϕ and ψ) and χ_1 and χ_2 torsion angle constraints were obtained using TALOS³⁶ and quantitative J-correlation spectroscopy³⁷, respectively. Residual HN dipolar couplings were measured using in-phase and anti-phase ¹H-¹⁵N HSQC experiments³⁸ on both NMR samples with and without adding Pfl phage to ~15 mg ml⁻¹. Experimentally determined distance, torsion angle and residual dipolar coupling constraints (Table 2) were applied in a simulated annealing protocol using the NIH version³⁹ of XPLOR⁴⁰. An ensemble of 512 structures was generated, from which 100 structures with lowest XPLOR target function values

were selected. Structural figures were generated with MolMol⁴¹. Structures were analyzed with AQUA and PROCHECK-NMR⁴². For the final 100 structures, 87.1% of the residues were in the core and 10.3% in the additionally allowed regions of the Ramachandran plot.

Accession codes. Protein Data Bank: Coordinates of the 100 conformers of the NMR structure, with experimental distance and angle constraints, have been deposited with accession code 2AFF. Biomolecular Magnetic Resonance Data-bank (www.bmr.bwisc.edu): NMR assignments for the complex have been deposited with accession number 6748.

Note: Supplementary information is available at the Nature Structural & Molecular Biology Website.

ACKNOWLEDGMENTS

We thank Y. Yoneda (Osaka University, Osaka, Japan) for providing the hNIFK gene. This work was supported by NIH grants CA87031 and CA69472, by the Genomics Research Center, Taiwan (M.-D.T.) and the Intramural Research Program of the NIH, National Institute of Diabetes and Digestive and Kidney Diseases, and in part by the Intramural AIDS Targeted Antiviral Program of the Office of the Director (A.M.G.). We thank D. Garrett and F. Delaglio for software, J. Baber for technical support, the MS and Proteomics Facility of OSU for MS analyses and D. Vandre of OSU for help in growing HeLa cells.

COMPETING INTERESTS STATEMENT

The authors declare that they have no competing financial interests.

Published online at <http://www.nature.com/nsmb/>

Reprints and permissions information is available online at <http://npg.nature.com/reprintsandpermissions/>

- Gerdes, J., Schwab, U., Lemke, H. & Stein, H. Production of a mouse monoclonal antibody reactive with a human nuclear antigen associated with cell proliferation. *Int. J. Cancer* **31**, 13–20 (1983).
- Gerdes, J. *et al.* Cell cycle analysis of a cell proliferation-associated human nuclear antigen defined by the monoclonal antibody Ki-67. *J. Immunol.* **133**, 1710–1715 (1984).
- Brown, D.C. & Gatter, K.C. Ki67 protein: the immaculate deception? *Histopathology* **40**, 2–11 (2002).
- Scholzen, T. & Gerdes, J. The Ki-67 protein: from the known and the unknown. *J. Cell Physiol.* **182**, 311–22 (2000).
- Schluter, C. *et al.* The cell proliferation-associated antigen of antibody Ki-67: a very large, ubiquitous nuclear protein with numerous repeated elements, representing a new kind of cell cycle-maintaining proteins. *J. Cell Biol.* **123**, 513–522 (1993).
- MacCallum, D.E. & Hall, P.A. The biochemical characterization of the DNA binding activity of pKi67. *J. Pathol.* **191**, 286–298 (2000).
- Endl, E. & Gerdes, J. Posttranslational modifications of the Ki-67 protein coincide with two major checkpoints during mitosis. *J. Cell. Physiol.* **182**, 371–380 (2000).
- Scholzen, T. *et al.* The Ki-67 protein interacts with members of the heterochromatin protein 1 (HP1) family: a potential role in the regulation of higher-order chromatin structure. *J. Pathol.* **196**, 135–144 (2002).
- Liao, H., Byeon, I.J. & Tsai, M.D. Structure and function of a new phosphopeptide-binding domain containing the FHA2 of Rad53. *J. Mol. Biol.* **294**, 1041–1049 (1999).
- Durocher, D., Henckel, J., Fersht, A.R. & Jackson, S.P. The FHA domain is a modular phosphopeptide recognition motif. *Mol. Cell* **4**, 387–394 (1999).
- Durocher, D. *et al.* The molecular basis of FHA domain:phosphopeptide binding specificity and implications for phospho-dependent signaling mechanisms. *Mol. Cell* **6**, 1169–1182 (2000).
- Liao, H. *et al.* Structure of the FHA1 domain of yeast Rad53 and identification of binding sites for both FHA1 and its target protein Rad9. *J. Mol. Biol.* **304**, 941–951 (2000).
- Li, J., Lee, G.I., Van Doren, S.R. & Walker, J.C. The FHA domain mediates phospho-protein interactions. *J. Cell Sci.* **113**, 4143–4149 (2000).
- Lee, G.I., Ding, Z., Walker, J.C. & Van Doren, S.R. NMR structure of the forkhead-associated domain from the *Arabidopsis* receptor kinase-associated protein phosphatase. *Proc. Natl. Acad. Sci. USA* **100**, 11261–11266 (2003).
- Schultz, J., Milpetz, F., Bork, P. & Ponting, C.P. SMART, a simple modular architecture research tool: identification of signaling domains. *Proc. Natl. Acad. Sci. USA* **95**, 5857–5864 (1998).
- Sueishi, M., Takagi, M. & Yoneda, Y. The forkhead-associated domain of Ki-67 antigen interacts with the novel kinesin-like protein Hklp2. *J. Biol. Chem.* **275**, 28888–28892 (2000).
- Takagi, M., Sueishi, M., Saiwaki, T., Kametaka, A. & Yoneda, Y. A novel nucleolar protein, NIFK, interacts with the forkhead associated domain of Ki-67 antigen in mitosis. *J. Biol. Chem.* **276**, 25386–25391 (2001).
- Li, H., Byeon, I.J., Ju, Y. & Tsai, M.D. Structure of human Ki67 FHA domain and its binding to a phosphoprotein fragment from hNIFK reveal unique recognition sites and

- new views to the structural basis of FHA domain functions. *J. Mol. Biol.* **335**, 371–381 (2004).
19. Pike, B.L., Yongkiettrakul, S., Tsai, M.D. & Heierhorst, J. Mdt1, a novel Rad53 FHA1 domain-interacting protein, modulates DNA damage tolerance and G(2)/M cell cycle progression in *Saccharomyces cerevisiae*. *Mol. Cell. Biol.* **24**, 2779–2788 (2004).
 20. Zhao, H., Tanaka, K., Nogochi, E., Nogochi, C. & Russell, P. Replication checkpoint protein Mrc1 is regulated by Rad3 and Tel1 in fission yeast. *Mol. Cell. Biol.* **23**, 8395–8403 (2003).
 21. Lee, S.J., Schwartz, M.F., Duong, J.K. & Stern, D.F. Rad53 phosphorylation site clusters are important for Rad53 regulation and signaling. *Mol. Cell. Biol.* **23**, 6300–6314 (2003).
 22. Cerosaletti, K.M. & Concannon, P. Nibrin forkhead-associated domain and breast cancer C-terminal domain are both required for nuclear focus formation and phosphorylation. *J. Biol. Chem.* **278**, 21944–21951 (2003).
 23. Stavridi, E.S. *et al.* Crystal structure of the FHA domain of the Chfr mitotic checkpoint protein and its complex with tungstate. *Structure* **10**, 891–899 (2002).
 24. Li, J. *et al.* Structural and functional versatility of the FHA domain in DNA-damage signaling by the tumor suppressor kinase Chk2. *Mol. Cell* **9**, 1045–1054 (2002).
 25. Yuan, C., Yongkiettrakul, S., Byeon, I.J., Zhou, S. & Tsai, M.D. Solution structures of two FHA1-phosphothreonine peptide complexes provide insight into the structural basis of the ligand specificity of FHA1 from yeast Rad53. *J. Mol. Biol.* **314**, 563–575 (2001).
 26. Byeon, I.J., Yongkiettrakul, S. & Tsai, M.D. Solution structure of the yeast Rad53 FHA2 complexed with a phosphothreonine peptide pTXXL: comparison with the structures of FHA2-pYXL and FHA1-pTXXD complexes. *J. Mol. Biol.* **314**, 577–588 (2001).
 27. Skurat, A.V. & Roach, P.J. Phosphorylation of sites 3a and 3b (Ser640 and Ser644) in the control of rabbit muscle glycogen synthase. *J. Biol. Chem.* **270**, 12491–12497 (1995).
 28. Wang, P. *et al.* II. Structure and specificity of the interaction between the FHA2 domain of Rad53 and phosphotyrosyl peptides. *J. Mol. Biol.* **302**, 927–940 (2000).
 29. Mahajan, A. *et al.* FHA domain-ligand interactions: importance of integrating chemical and biological approaches. *J. Am. Chem. Soc.* published online 30 September 2005 (doi: 10.1021/ja054538m).
 30. Clore, G.M. & Gronenborn, A.M. Determining the structures of large proteins and protein complexes by NMR. *Trends Biotechnol.* **16**, 22–34 (1998).
 31. Bax, A. & Grzesiek, S. Methodological advances in protein NMR. *Acc. Chem. Res.* **26**, 131–138 (1993).
 32. Lee, W., Revington, M.J., Arrowsmith, C. & Kay, L.E. A pulsed field gradient isotope-filtered 3D ¹³C HMQC-NOESY experiment for extracting intermolecular NOE contacts in molecular complexes. *FEBS Lett.* **350**, 87–90 (1994).
 33. Ikura, M. & Bax, A. Isotope-filtered 2D NMR of a protein-peptide complex: study of a skeletal muscle myosin light chain kinase fragment bound to calmodulin. *J. Am. Chem. Soc.* **114**, 2433–2440 (1992).
 34. Delaglio, F. *et al.* NMRPipe: a multidimensional spectral processing system based on UNIX pipes. *J. Biomol. NMR* **6**, 277–293 (1995).
 35. Garrett, D.S., Powers, R., Gronenborn, A.M. & Clore, G.M.A. Common-sense approach to peak picking in 2-dimensional, 3-dimensional, and 4-dimensional spectra using automatic computer-analysis of contour diagrams. *J. Magn. Reson.* **95**, 214–220 (1991).
 36. Cornilescu, G., Delaglio, F. & Bax, A. Protein backbone angle restraints from searching a database for chemical shift and sequence homology. *J. Biomol. NMR* **13**, 289–302 (1999).
 37. Bax, A. *et al.* Measurement of homo- and heteronuclear J couplings from quantitative J correlation. *Methods Enzymol.* **239**, 79–105 (1994).
 38. Ottiger, M., Delaglio, F. & Bax, A. Measurement of J and dipolar couplings from simplified two-dimensional NMR spectra. *J. Magn. Reson.* **131**, 373–378 (1998).
 39. Schwieters, C.D., Kuszewski, J.J., Tjandra, N. & Clore, G.M. The XPLOR-NIH NMR molecular structure determination package. *J. Magn. Reson.* **160**, 65–73 (2003).
 40. Brünger, A.T. *X-PLOR: a System for X-ray Crystallography and NMR*, xvii, 382 (Yale University Press, New Haven, Connecticut, 1992).
 41. Koradi, R., Billeter, M. & Wüthrich, K. MolMol: a program for display and analysis of macromolecular structures. *J. Mol. Graph* **14**, 29–32, 51–55 (1996).
 42. Laskowski, R.A., Rullmann, J.A.C., MacArthur, M.W., Kaptein, R. & Thornton, J.M. AQUA and PROCHECK-NMR: programs for checking the quality of protein structures solved by NMR. *J. Biomol. NMR* **8**, 477–486 (1996).